

V736 CEPHEI – AN A-TYPE OVERCONTACT BINARY

NELSON, ROBERT H.^{1,2}

¹ Mountain Ash Observatory, 1393 Garvin Street, Prince George, BC, Canada, V2M 3Z1
email: bob.nelson@shaw.ca

² Guest investigator, Dominion Astrophysical Observatory, Herzberg Institute of Astrophysics, National Research Council of Canada

The discoverer of the variability of V736 Cep (NSV 13635, NSVS 3275157, HD 235475, SAO 33275, TYC 3957-12-1) appears to be undocumented. As part of the HD catalogue, it was classified presumably by Cannon and Pickering (1993) as F8. The first relevant reference is to Otero et al. (2005) who provided coordinates, elements (epoch and period), apparent reference to the above classification, and an eclipse type (EA). Since then, there have been numerous eclipse timings published, but no light curve or analysis.

In order to rectify this lack, the author first secured, in September of 2011, 2013, 2014, and 2015, a total of 14 medium resolution ($R \sim 10000$ on average) spectra of V736 Cep at the Dominion Astrophysical Observatory (DAO) in Victoria, British Columbia, Canada using the Cassegrain spectrograph attached to the 1.85 m Plaskett Telescope. He used the 21181 configuration and a grating with 1800 lines/mm, blazed at 5000 Å, and giving a reciprocal linear dispersion of 10 Å/mm in the first order. The wavelengths ranged from 5000 to 5260 Å, approximately. A log of observations is given in Table 1 and an eclipse timing diagram, in Figure 9 later in the paper. The following elements were used for both radial velocity (RV) and photometric phasing:

$$\text{JD (Hel) Min I} = 2457619.7380 + 0.8578464E \quad (1)$$

Frame reduction was performed by software RaVeRe (Nelson 2013). See Nelson (2010) and Nelson et al. (2014) for further details. The normalized spectra are reproduced in Fig. 1, sorted by phase. Note towards the right the strong neutral iron lines (at 5167.487 and 5171.595 Å) and the strong neutral magnesium triplet (at 5167.33, 5172.68, and 5183.61 Å).

Radial velocities were determined using the Rucinski broadening functions (Rucinski, 2004, Nelson, 2010) as implemented in software Broad25 (Nelson, 2013). See Nelson et al. (2014) for further details. An Excel worksheet with built-in macros (written by him) was used to do the necessary radial velocity conversions to geocentric and back to heliocentric values (Nelson 2014). The resulting RV determinations are also presented in Table 1. The mean rms errors for RV_1 and RV_2 are 5.9 and 6.9 km/s, respectively, and the overall rms deviation from the (sinusoidal) curves of best fit is 9.1 km/s. The best fit yielded the values $K_1 = 49.8$ (1.7) km/s, $K_2 = 251.1$ (2.3) km/s and $V_\gamma = -12.4$ (1.4) km/s, and thus a mass ratio $q_{\text{sp}} = K_1/K_2 = M_2/M_1 = 0.198$ (7).

Table 1: Log of DAO observations.

DAO Image#	Mid Time (HJD-2400000)	Exposure (sec)	Phase at Mid-exp	V_1 (km/s)	V_2 (km/s)
11-08068	55815.9293	3600	0.282	-71.5 (5.8)	224.5 (5.8)
11-08086	55816.7831	3600	0.278	-57.1 (7.3)	236.9 (13.4)
11-08169	55823.9181	3600	0.595	13.1 (5.0)	—
11-08200	55824.9408	3600	0.787	38.8 (5.7)	-239.6 (4.0)
11-08211	55825.7162	3600	0.691	29.3 (4.3)	-242.3 (4.1)
11-08214	55825.7657	3600	0.749	11.7 (4.8)	-268.6 (3.8)
13-09667	56545.9245	3600	0.245	-60.2 (5.2)	249.2 (10.7)
14-24341	56906.7363	1200	0.847	26.5 (5.8)	-224.1 (5.4)
14-24403	56908.7899	1200	0.241	-70.5 (4.1)	—
14-24415	56908.8968	1200	0.365	-43.7 (9.1)	176.2 (12.6)
15-13014	57291.8559	1200	0.785	39.7 (5.6)	-247.1 (3.5)
15-13015	57291.8736	1800	0.805	43.2 (8.0)	-250.9 (4.8)
15-13128	57295.6376	3600	0.193	-68.8 (6.1)	238.4 (7.0)
15-12130	57295.6697	1800	0.230	-64.3 (6.0)	237.2 (8.2)

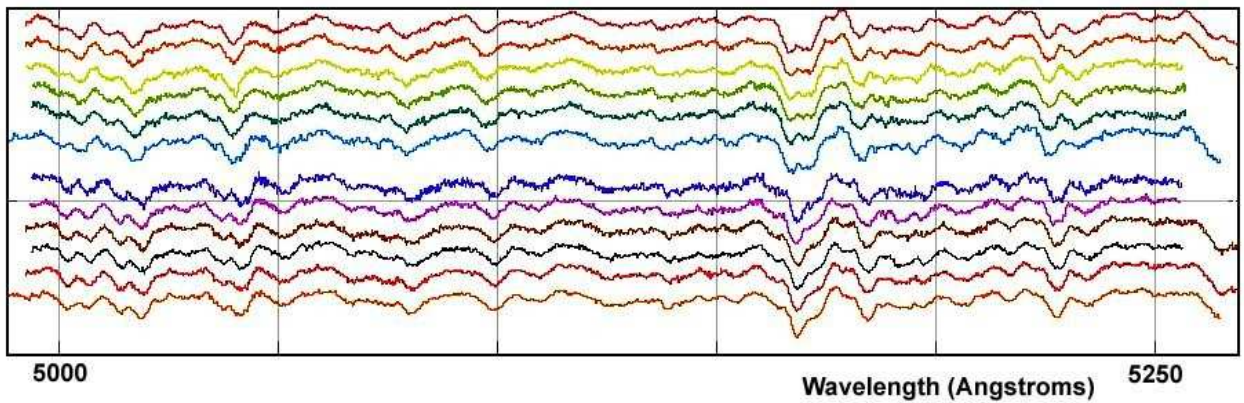


Figure 1. V736 Cep spectra at phases 0.193, 0.230, 0.245, 0.278, 0.282, 0.365, 0.691, 0.749, 0.785, 0.787, 0.805, 0.847 (from top to bottom).

Representative broadening functions, at phases 0.232 and 0.778 are depicted in Figs. 2 and 3, respectively. Smoothing by a Gaussian filter is routinely done in order to centroid the peak values for determining the radial velocities.

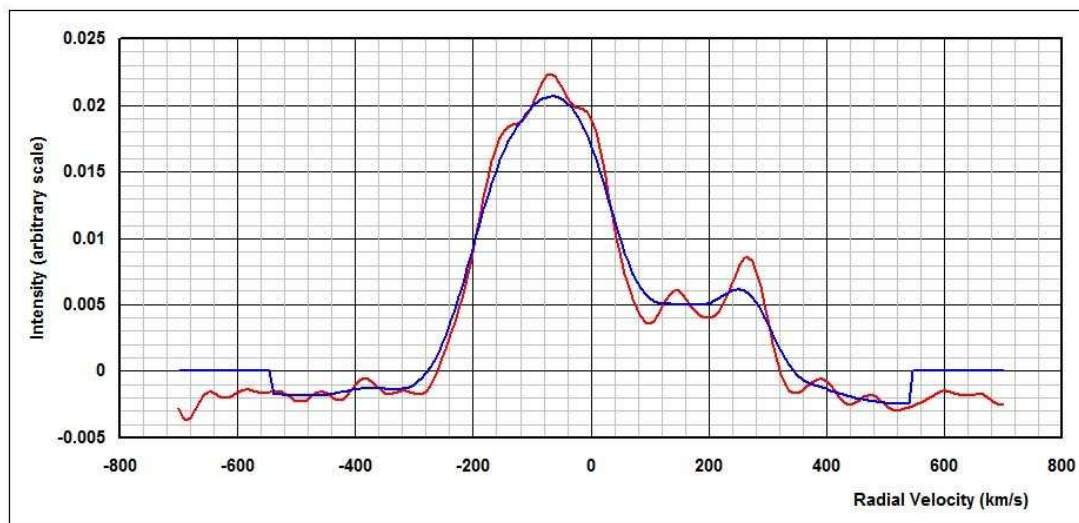


Figure 2. Broadening functions at phase 0.230—smoothed and unsmoothed.

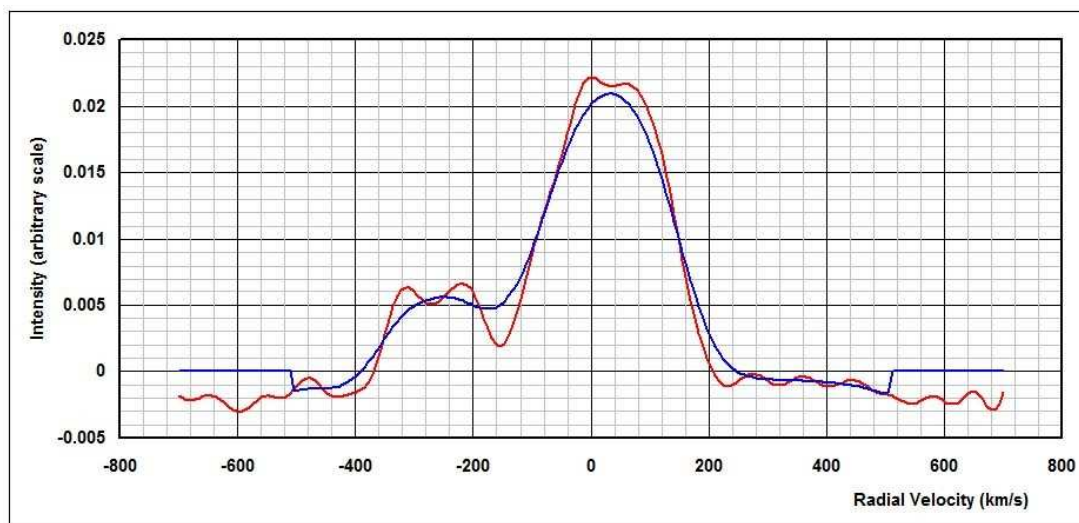


Figure 3. Broadening functions at phase 0.785—smoothed and unsmoothed.

In the autumn months of 2015 and 2016 the author took a total of 269 frames in V , 277 in R_C (Cousins) and 277 in the I_C (Cousins) band at his private observatory in Prince George, B.C., Canada. Renamed Mountain Ash Observatory, it is the former Sylvester Robotic Observatory described in Nelson (2009). A finder chart is included as Fig. 10 at the end of the paper.

Standard reductions were then applied (see Nelson et al., 2014 for more details). The variable, comparison and check stars are listed in Table 2. The coordinates and magnitudes for V736 Cep, the comparison, and check stars are from the Tycho Catalogue, Hog,

Table 2: Details of variable, comparison and check stars.

Object	GSC	RA (J2000)	Dec (J2000)	V (mag)	$B - V$ (mag)
Variable	3957-0012	21 ^h 16 ^m 29 ^s .1133	+55°23′10″.236	9.82 (3)	+0.40 (4)
Comparison	3957-0898	21 ^h 17 ^m 29 ^s .8881	+55°33′32″.048	10.10 (3)	+0.87 (7)
Check	3957-0310	21 ^h 17 ^m 07 ^s .2846	+55°23′03″.045	10.66 (5)	+0.34 (7)

Table 3: Limb darkening values from Van Hamme (1993).

Band	x_1	x_2	y_1	y_2
Bol	0.645	0.644	0.227	0.226
V	0.735	0.739	0.263	0.259
R_C	0.662	0.667	0.274	0.272
I_C	0.579	0.583	0.265	0.264

et al., (2000), and converted to standard Johnson values using relations due to Henden (2001).

The author used the 2003 version of the Wilson-Devinney (WD) light curve and radial velocity analysis program with the Kurucz atmospheres (Wilson and Devinney, 1971, Wilson, 1990, Kallrath and Milone, 1998, Wilson, 1998) as implemented in the Windows front-end software WDwint (Nelson, 2013) to analyse the data. To get started, the spectral type F8 (taken from SIMBAD, no reference given; but there is an implied reference to Cannon and Pickering (1993) in Otero et al. (2005). Interpolated tables from Flower (1996) gave a temperature $T_1 = 6199 \pm 120$ K and $\log g = 4.367 \pm 0.004$. (The quoted errors refer to one spectral sub-class.) An interpolation program by Terrell (1994, available from Nelson 2013) gave the Van Hamme (1993) limb darkening values; and finally, a logarithmic (LD=2) law for the limb darkening coefficients was selected, appropriate for temperatures < 8500 K (ibid.). The limb darkening coefficients are listed in Table 3. (The values for the second star are based on the later-determined temperature of 6101 K and assumed spectral type of F8-9.) Convective envelopes for both stars were used, appropriate for cooler stars (hence values gravity exponent $g = 0.32$ and albedo $A = 0.500$ were used for each).

From the GCVS 4 designation (EW) and from the shape of the light curve, mode 3 (overcontact binary) mode was used.

Convergence was attempted by the method of multiple subsets. The subsets were: (a, V_γ, i, L_1) , (T_2, Ω_1) , and (q, L_1) . However, no reasonable fit could be obtained until a spot was placed on the back side of star 1 (visible during secondary minimum). Thereafter, the fitting proceeded smoothly.

Detailed reflections were tried, with $n_{\text{ref}} = 3$, but there was little—if any—difference in the fit from the simple treatment. There are certain uncertainties in the process (see Csizmadia et al., 2013, Kurucz, 2000). On the other hand, the solution is very weakly dependent on the exact values used.

The model is presented in Table 4. For the most part, the error estimates are those provided by the WD routines and are known to be low; however, it is a common practice to quote these values and we do so here. Also, estimating the uncertainties in temperatures T_1 and T_2 is somewhat problematic. A common practice is to quote the temperature difference over—say—one spectral sub-class (assuming that the classification is good to one spectral sub-class, the precision being unknown in this case). In addition, various different calibrations have been made (Cox, 2000, page 388-390 and references therein, and Flower, 1996), and the variations between the various calibrations can be significant. If the

classification is \pm one sub-class, an uncertainty of ± 120 K to the absolute temperatures of each, would be reasonable. The modelling error in temperature T_2 , relative to T_1 , is indicated by the WD output to be much smaller, around 7 K.

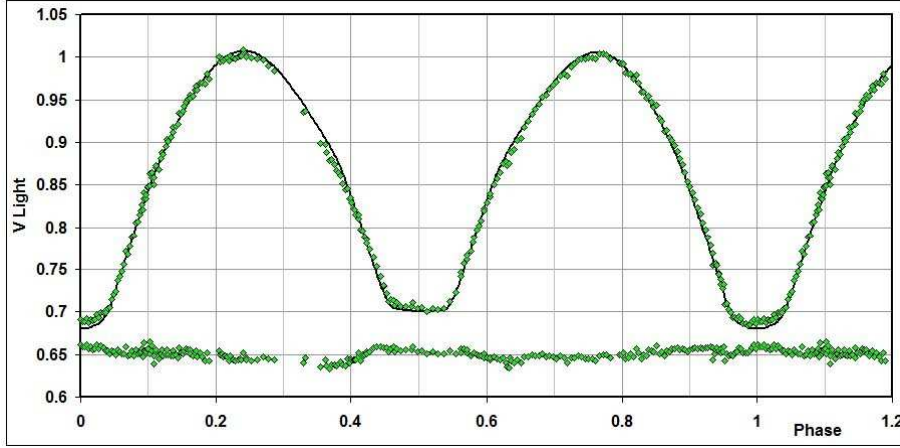


Figure 4. *V* light curves for V736 Cep – data, WD fit, and residuals.

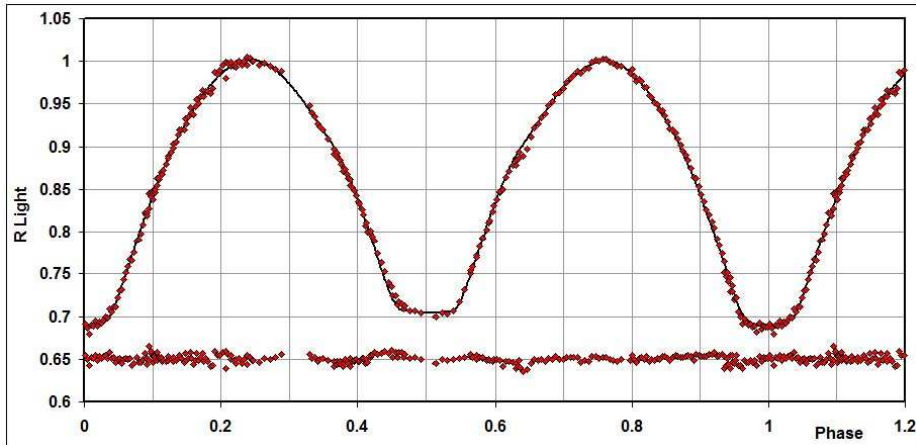


Figure 5. *R* light curves for V736 Cep – data, WD fit, and residuals.

The light curve data and the fitted curves are depicted in Figures 4-6. The residuals (in the sense observed-calculated) are also plotted, shifted upwards by 0.65 units.

The radial velocities are shown in Fig. 7. A three-dimensional representation from Binary Maker 3 (Bradstreet, 1993) is shown in Fig. 8.

The WD output fundamental parameters and errors are listed in Table 5. Most of the errors are output or derived estimates from the WD routines. From Kallrath & Milone (1998), the fill-out factor is $f = (\Omega_I - \Omega)/(\Omega_I - \Omega_O)$, where Ω is the modified Kopal potential of the system, Ω_I is that of the inner Lagrangian surface, and Ω_O , that of the outer Lagrangian surface, was also calculated.

To determine the distance, the analysis proceeded as follows: First the WD routine gave the absolute bolometric magnitudes of each component; these were then converted

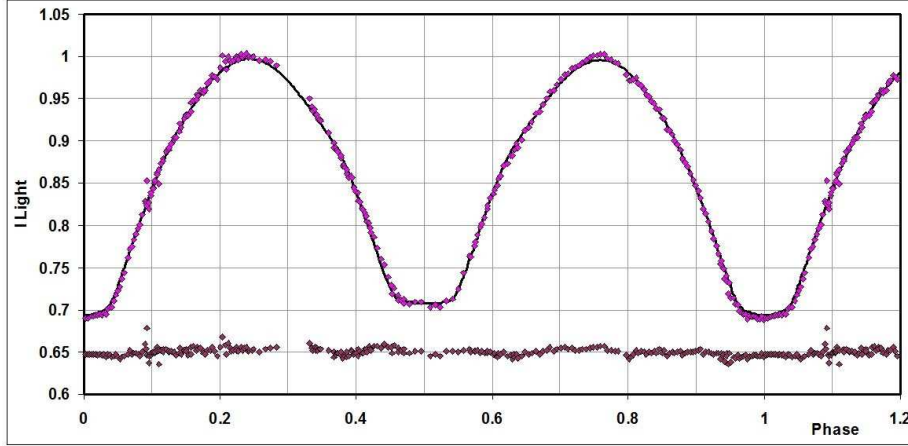


Figure 6. I light curves for V736 Cep – data, WD fit, and residuals.

Table 4: Wilson-Devinney parameters.

WD Quantity	Value	error	Unit
Temperature, T_1	6199	[fixed]	K
Temperature, T_2	6101	120	K
$q = m_2/m_1$	0.189	0.001	—
Potential, $\Omega_1 = \Omega_2$	2.152	0.002	—
Inclination, i	80.68	0.17	degrees
Semi-maj. axis, a	5.23	0.06	solar radii.
V_γ	-13.4	1.8	km/s
Fill-out, f_1	0.431	0.024	
Spot co-latitude	70	5	degrees
Spot longitude	171	2	degrees
Spot radius	17.2	0.5	degrees
Spot temp. factor	0.948	0.004	
$L_1/(L_1 + L_2)$ (V)	0.8203	0.0002	—
$L_1/(L_1 + L_2)$ (R_{CC})	0.8188	0.0001	—
$L_1/(L_1 + L_2)$ (I_{CC})	0.8174	0.0001	—
r_1 (pole)	0.5041	0.0004	orbital radii
r_1 (side)	0.5541	0.0007	orbital radii.
r_1 (back)	0.5803	0.0009	orbital radii
r_2 (pole)	0.2434	0.0011	orbital radii
r_2 (side)	0.2553	0.0014	orbital radii
r_2 (back)	0.3038	0.0033	orbital radii.
Phase shift	0.0004	0.0001	—
$\Sigma\omega_{res}^2$	0.07958	—	—

Table 5: Fundamental parameters.

Quantity	Value	Error	unit
Temperature, T_1	6199	120	K
Temperature, T_2	6101	120	K
Mass, m_1	2.20	0.06	M0
Mass, m_2	0.41	0.02	M0
Radius, R_1	2.86	0.01	R0
Radius, R_2	1.40	0.01	R0
$M_{\text{bol},1}$	2.20	0.02	mag
$M_{\text{bol},2}$	3.82	0.02	mag
$\log g_1$	3.87	0.01	cgs
$\log g_2$	3.76	0.01	cgs
Luminosity, L_1	10.9	0.2	L0
Luminosity, L_2	2.44	0.05	L0
Fill-out factor 1,2	0.43	0.02	—
Distance, r	316	6	pc

to the absolute visual (V) magnitudes of both, $M_{V,1}$ and $M_{V,2}$, using the bolometric corrections $BC = -0.160$ and -0.17 for stars 1 and 2 respectively. The latter were taken from interpolated tables constructed from Cox (2000). The absolute V magnitude was then computed in the usual way, getting $M_V = 2.14 \pm 0.02$ magnitudes. The apparent magnitude in the V passband was $V = 9.854 \pm 0.03$, taken from the Tycho values (Hog et al. 2000) and converted to the Johnson magnitude 9.816 ± 0.03 using relations due to Henden (2001).

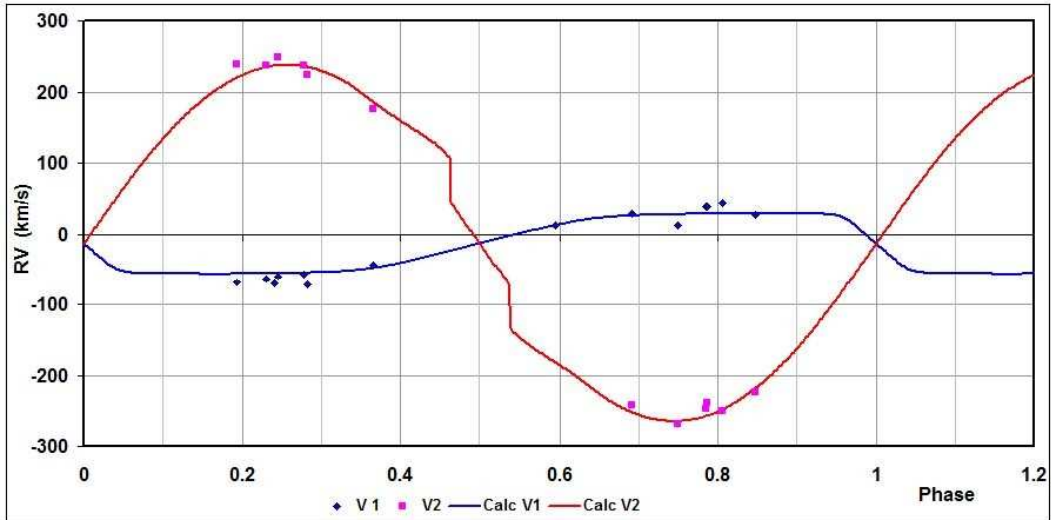


Figure 7. Radial velocity curves for V736 Cep – data and WD fit.

Ignoring interstellar absorption (setting $A_V = 0$), we calculated a preliminary value for the distance $r = 343$ pc from the standard relation:

$$r = 10^{0.2(V - M_V - A_V + 5)} \text{ parsecs} \quad (2)$$

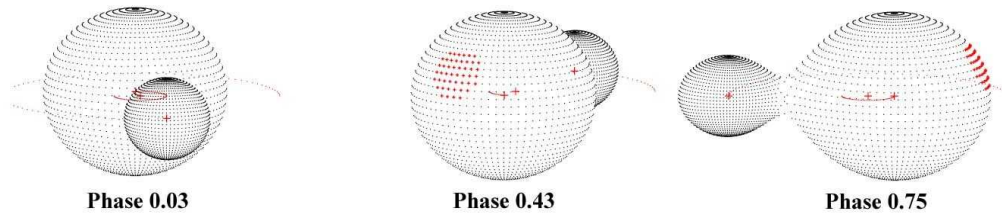


Figure 8. Binary Maker 3 representation of the system – at phases 0.03, 0.43 and 0.75.

Galactic extinction was obtained from a model by Amôres & Lépine (2005). The code (available in IDL and converted by the author to a Visual Basic routine) assumes that the interstellar dust is well mixed with the dust, that the galaxy is axi-symmetric, that the gas density in the disk is a function of the Galactic radius and of the distance from the Galactic plane, and that extinction is proportional to the column density of the gas. Using Galactic coordinates of $l = 95^{\circ}5859$ and $b = +4^{\circ}3732$ (SIMBAD), and the initial distance estimate of $d = 0.343$ kpc, a value of $A_V = 0.175$ magnitude was determined. A further iteration revealed little change in A_V . Substitution into (2) gave $r = 316$ pc.

The errors were assigned as follows: $\delta M_{\text{bol},1} = \delta M_{\text{bol},2} = 0.02$, $\delta BC_1 = \delta BC_2 = 0.009$ (the variation of 1 spectral sub-class), $\delta V = 0.03$, $\delta A_V = 0.01$, all in magnitudes. Combining the errors rigorously (i.e., by adding the variances) yielded an estimated error in r of 6 pc which is probably far too low.

Some comments regarding the period variation are in order. An eclipse timing difference (O–C) plot using timings from 1999 is depicted in Fig. 9. Although there is considerable scatter, a linear relation over the interval, cycle 4400 (in 2009) to cycle 7380 (in 2016) was determined. This yielded a best-fit linear solution and ephemeris of Equation (1) above.

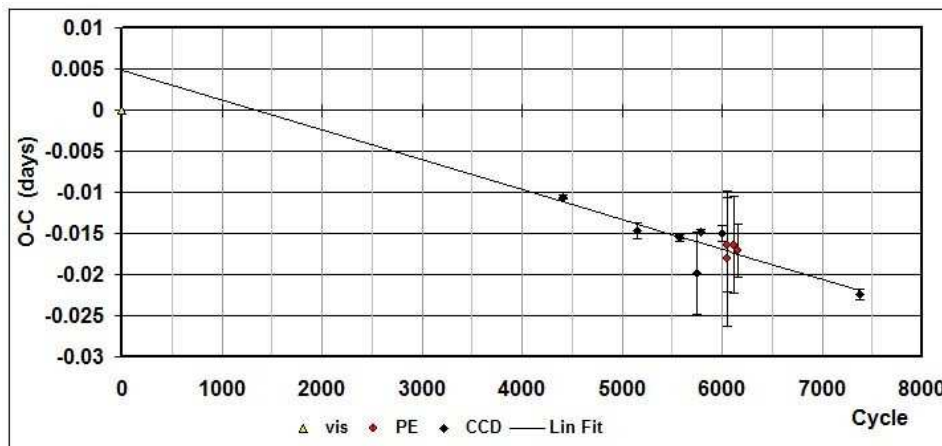


Figure 9. V736 Cep – eclipse timing (O–C) diagram with a linear fit for points after cycle 4000.

In conclusion, all the fundamental parameters for V736 Cephei have been determined. It will be interesting to monitor this system photometrically in the coming years to observe the evolution of the spot.

The Excel file (and many others) are available at Nelson (2016). The 8000+ files are

updated annually.

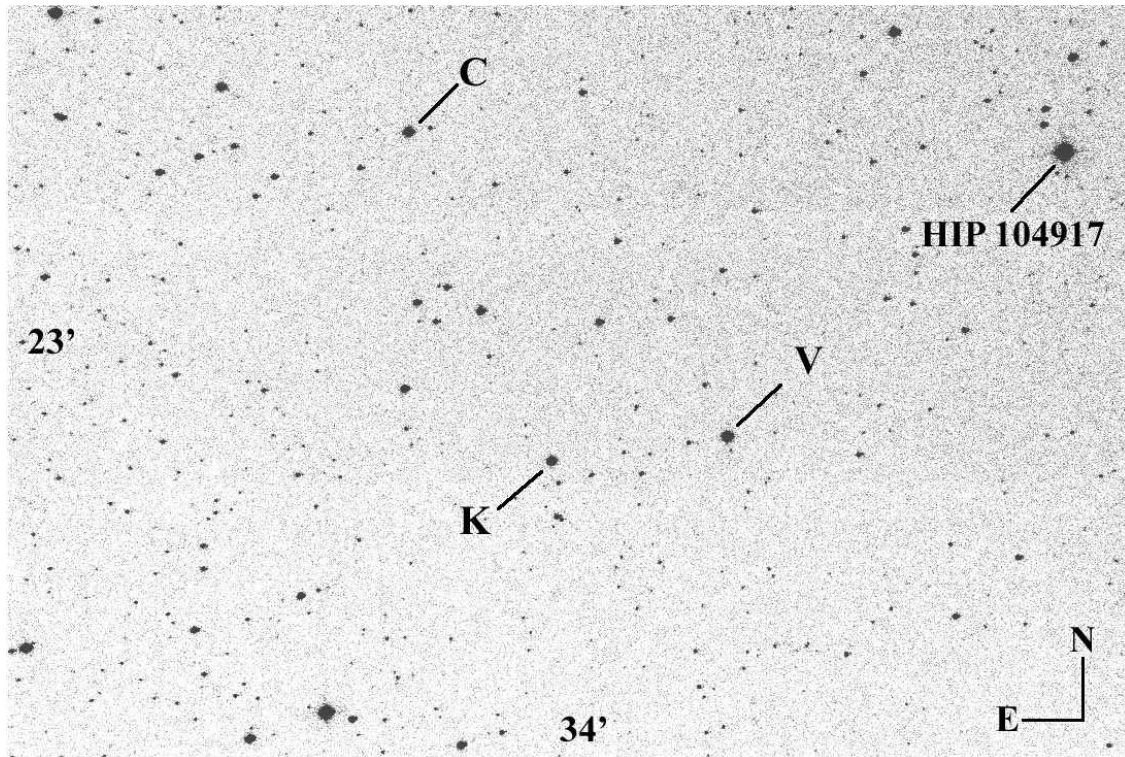


Figure 10. Sample CCD frame of the field of view showing the stars of interest.

Acknowledgements: It is a pleasure to thank the staff members at the DAO (Dmitry Monin, David Bohlender, and the late Les Suddlmyer) for their usual splendid help and assistance. Much use was made of the SIMBAD database during this research.

References:

- Amôres, E.B., Lépine, J.R.D., 2005, *AJ*, **130**, 659 DOI
- Bradstreet, D.H., 1993, “Binary Maker 2.0 - An Interactive Graphical Tool for Preliminary Light Curve Analysis”, in Milone, E.F. (ed.) *Light Curve Modelling of Eclipsing Binary Stars*, pp 151-166 (Springer, New York, N.Y.) DOI
- Cannon, A.J., Pickering, E.C., 1993, *Harv. Ann.*, 91-100 (1918-1924; ADC 1989), *Henry Draper Catalogue and Extension 1 (HD, HDE)*
- Cox, A.N., ed, 2000, *Allen’s Astrophysical Quantities*, 4th ed., (Springer, New York, NY) DOI
- Csizmadia, S., Pasternacki, T., Dreyer, C., Cabrera, A., Erikson, A., Rauer, H., 2013, *A&A*, **549**, A9 DOI
- Flower, P.J., 1996, *ApJ*, **469**, 355 DOI
- Henden, A., 2001, <http://www.tass-survey.org/tass/catalogs/tycho.old.html>
- Hog, E., et al., 2000, *A&A*, **355**, L27

- Kallrath, J., Milone, E.F., 1998, *Eclipsing Binary Stars—Modeling and Analysis* (Springer-Verlag). DOI
- Kurucz, R.L., 2000, *BaltA*, **11**, 101
- Nelson, R.H., 2009, *IBVS*, **5884**
- Nelson, R.H., 2010, “Spectroscopy for Eclipsing Binary Analysis” in *The Alt-Az Initiative, Telescope Mirror & Instrument Developments* (Collins Foundation Press, Santa Margarita, CA), R.M. Genet, J.M. Johnson and V. Wallen (eds) [available on ResearchGate]
- Nelson, R.H., 2013, Software by Bob Nelson,
<https://www.variablestarssouth.org/bob-nelson/>
- Nelson, R.H., 2014, Spreadsheets, by Bob Nelson,
<https://www.variablestarssouth.org/bob-nelson/>
- Nelson, R.H., 2016, Bob Nelson’s *O–C* Files, <http://www.aavso.org/bob-nelsons-o-c-files>
- Nelson, R.H., Şenavci, H.V., Baştürk, Ö, and Bahar, E., 2014, *NewA*, **29**, 57 DOI
- Otero, S.A., Wils, P, and Dubovsky, P.A., 2005, *IBVS*, **5586**
- Rucinski, S. M., 2004, “Advantages of the Broadening Function (BF) over the Cross-Correlation Function (CCF)”, in *Stellar Rotation, Proc. IAU Symp.*, **215**, 17
- Terrell, D., 1994, *Van Hamme Limb Darkening Tables*, vers. 1.1.
- Van Hamme, W., 1993, *AJ*, **106**, 2096 DOI
- Wilson, R.E., 1990, *ApJ*, **356**, 613 DOI
- Wilson, R.E., 1998, *Documentation of Eclipsing Binary Computer Model* (available from the author)
- Wilson, R.E., and Devinney, E.J., 1971, *ApJ*, **166**, 605 DOI